JACS
JOURNAL OF THE AMERICAN CHEMICAL SOCIETY

ARTICLE

pubs.acs.org/JACS

Single-Conformation Ultraviolet and Infrared Spectra of Jet-Cooled Monolignols: *p*-Coumaryl Alcohol, Coniferyl Alcohol, and Sinapyl Alcohol

Chirantha P. Rodrigo, William H. James, III, and Timothy S. Zwier*

Department of Chemistry, Purdue University, West Lafayette, Indiana 47907-2084, United States

Supporting Information

ABSTRACT: Single-conformation spectroscopy of the three lignin monomers (hereafter "monolignols") *p*-coumaryl alcohol (*p*CoumA), coniferyl alcohol (ConA), and sinapyl alcohol (SinA) has been carried out on the isolated molecules cooled in a supersonic expansion. Laser-induced fluorescence excitation, dispersed fluorescence, resonant two-photon ionization, UV−UV hole-burning, and resonant ion-dip infrared spectroscopy were carried out as needed to obtain firm assignments for the observed conformers of the three molecules. In each case, two conformers were observed, differing in the relative orientations of the vinyl and OH substituents para to one another on the phenyl ring. In *p*CoumA, the two conformers have S_0-S_1 origins nearly identical in size, split from one another by only 7 cm^{-1}, in close analogy with previous results of Morgan et al. on *p*-vinylphenol (*Chem. Phys.* **2008**, *347*, 340). ConA, with its methoxy group ortho to the OH group, also has two low-energy conformers forming a *syn*/*anti* pair, in this case with the OH group locked into an orientation in which it forms an intramolecular H-bond with the adjacent methoxy group. The electronic frequency shift between the two conformers is dramatically increased to 805 cm^{-1}, with the dominant conformer of ConA (with S_0-S_1 origin at 32 640 cm^{-1}) about 5 times the intensity of its minor counterpart (with S_0-S_1 origin at 33 444 cm^{-1}). The presence of an $OH\cdots OCH_3$ intramolecular H-bond is established by the shift of the OH stretch fundamental of the OH group to 3599 cm^{-1}, as it is in *o*-methoxyphenol (Fujimaki et al. *J. Chem. Phys.* **1999**, *110*, 4238). Analogous single-conformation UV and IR spectra of *o*-methoxy-*p*-vinylphenol show a close similarity to ConA and provide a basis for a firm assignment of the red-shifted (blue-shifted) conformer of both molecules to the *syn* (*anti*) conformer. The two observed conformers of SinA, with its two methoxy group straddling the OH group, have S_0-S_1 origins split by 239 cm^{-1} (33 055 and 33 294 cm^{-1}), a value between those in *p*CoumA and ConA. A combination of experimental data and calculations on the three monolignols and simpler derivatives is used to establish that the conformational preferences of the monolignols reflect the preferences of each of the ring substituents separately, enhanced by the presence of the intramolecular $OH\cdots OCH_3$ H-bond. Taken as a whole, the presence of multiple flexible substituents locks in certain preferred orientations of the groups relative to one another, even in the apparently flexible allyl alcohol side chain ($-CH{=}CH-CH_2OH$), where the OH group orients itself so that the hydrogen is pointed back over the vinyl π cloud in order to minimize interactions between the oxygen lone pairs and the π electrons.

1. INTRODUCTION

Lignin is an abundant natural product found in the cell walls of all vascular plants.[1,2] The presence of lignin in the cell walls provides crucial strength and rigidity to the plant and protection against attack by microorganisms on the cellulose and hemicellulose core.[3] The very different structural requirements of lignin in different plants ranging from grasses to the largest of trees are controlled by changes in the stoichiometric proportions of just three monolignols,[1,3] *p*-coumaryl alcohol (*p*CoumA), coniferyl alcohol (ConA), and sinapyl alchol (SinA), whose structures are shown in parts a, b, and c of Figure 1, respectively. The final lignin product in the cell wall is produced by oxidative radical[4,5] coupling of these monomer units, with many of the structural properties dictated by the variety of chemically distinct linkages between them.[1,6] Of the three monomers, ConA is pervasive in all plants[7] and is the main constituent of soft wood, while both ConA and SinA are common in hardwoods,[6] where their presence provides greater structural integrity through cross-linking of the lignin oligomer chains. Herbaceous plants (with no woody stem above the ground) contain the third monomer, *p*CoumA.[6]

One of the important challenges facing biofuel production is understanding and controlling the properties of lignin in order to increase the efficiency with which it can be broken down during biofuel extraction and converted into useful products.[8,9] The present study of the single-conformation spectroscopy of the monolignols provides a useful starting point for future spectroscopic studies of larger lignin oligomers that determine the spectral signatures of the various chemical linkages between monomer units. Furthermore, the monolignols are in themselves an important constituent of plants, being synthesized and transported to the cell walls either as the monolignols themselves or as glucoside derivatives.[10−12]

Received: October 13, 2010
Published: February 4, 2011

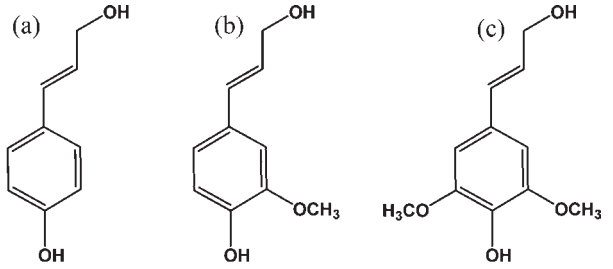

p-coumaryl alcohol | coniferyl alcohol | sinapyl alcohol

Figure 1. Chemical structures of the three monomeric lignin precursor molecules (lignols).

While there are no previous reports of the gas-phase spectra of the monolignols, there are previous studies of three close analogues, *p*-vinylphenol (*p*VP),[13,14] *p*-coumaric acid (*p*CA),[15] and *o*-methyoxyphenol (*o*MP),[16] that provide useful points of comparison. A theoretical investigation of the three monolignols both as stable neutrals and as radicals[17] has been reported, but the focus there was on the calculated properties of the global minimum conformers only.

Relative to many previous studies of the conformation-specific spectroscopy of biologically relevant molecules, one of the unique aspects of the three monolignols is that they are composed of multiple side chains of varying length and functionality attached to the same aromatic ring (OH, OCH_3, CH═CH−CH_2OH). Each of these groups has its own conformational preference when attached to the aromatic ring as a lone substituent. In addition, there is now the possibility of interactions between the substituents (e.g., intramolecular H-bonding and electronic effects mediated by the aromatic ring). The present study will use single-conformation UV and IR spectroscopy to establish the preferred conformations of the three monolignols. We will seek to determine the degree to which the local preferences of the individual substituents are retained in the monolignols or whether the presence of multiple substituents modifies these preferences and in what way. At the same time, the single-conformation methods employed here provide spectroscopic signatures of the low-energy conformations observed, providing a foundation for future studies of larger lignin oligomers.

2. EXPERIMENTAL AND COMPUTATIONAL METHODS

Jet-cooled laser spectroscopy employing both fluorescence and mass-resolved, resonant two-photon ionization (R2PI) detection schemes was used in this work. A detailed description of the fluorescence chamber[18] and molecular beam time-of-flight mass spectrometers[19] used here has been given elsewhere The supersonic expansions were produced using a pulsed valve (Parker series 9, 800 μm diameter) operating at 20 Hz. Samples, all solids at room temperature, were heated to appropriate temperatures in a sample reservoir located just behind the pulsed valve. Temperatures of 110 °C (*p*CoumA), 80[9]C (ConA), 95−120 °C (sinA), and 30 °C (MVP) were used to generate sufficient vapor pressure seeded in He carrier gas (2−4 bar) for expansion. Gas flow rates of 5−7 and 30−40 bar·cm^3/min were maintained for ion based and fluorescence based experiments, respectively. Samples of varying purity were purchased from commercial vendors (Table S1, Supporting Information) and used without further purification. All three monolignols underwent thermal polymerization/degradation, leading to loss of signal and the onset of interferences when fluorescence detection was used. The carriers of the transitions reported here were verified by mass resolved R2PI as needed.

In both detection schemes, the frequency doubled output of a Nd:YAG pumped dye laser was used for the ultraviolet photon. Typical laser powers of ∼0.1−0.2 mJ/pulse were employed. For FE spectroscopy, the total fluorescence signal was imaged onto a photomultiplier tube (PMT) collected at right angles to the laser axis and the laser frequency is tuned through the region of interest. Appropriate long wavelength pass filters (Schott glass) were used before the PMT to reduce the contribution from scattered laser light. One color R2PI spectra were recorded using a gently focused UV laser beam and collecting the molecular ions generated via R2PI.

Dispersed fluorescence (DFL) spectroscopy was used in making assignments of the observed vibronic spectra. In this case, the wavelength of the UV laser was fixed on a vibronic transition selected from the FE spectrum. The fluorescence was dispersed by a 3/4 m monochromoator (Jobin Yvon 750i) equipped with a CCD camera (Andor Technology, model DBU2U440).

UV−UV hole-burn (UVHB) spectroscopy and fluorescence dip IR spectroscopy (FDIRS) were utilized to record conformation specific ultraviolet and IR spectra, respectively.[19] In UVHB spectroscopy a relatively high powered UV laser firing at 10 Hz (0.2−0.4 mJ/pulse) has its wavelength fixed on a transition selected from the FE (or R2PI) spectrum. A second UV probe laser (0.1−0.2 mJ·$pulse^{-1}$), firing at 20 Hz, is spatially overlapped with the first and delayed from it by ∼200 ns. The probe laser is tuned through the frequency range of interest while the difference in probe laser signal (with and without hole-burn laser present) is recorded using active baseline subtraction in a gated integrator (Stanford Research SRS250).

Similarly, FDIR spectroscopy is carried out by replacing the UVHB laser with an IR laser beam. However, in this case the IR hole-burn laser is tuned while the ground state population of a given conformer is monitored with the UV probe laser. Whenever a hydride stretch absorption of that conformer is encountered, a fraction of the ground state zero-point level population is removed, producing a nonzero difference signal. The IR radiation was generated by an infrared parametric converter (LaserVision). The system is pumped with a seeded output of a Nd:YAG laser (Continuum, series 8000) with typical peak powers of 550 mJ·$pulse^{-1}$ (1064 nm, 10 Hz). The parametric converter was tuned through the range 2800−3750 cm^{-1} with peak power 2−3 mJ/pulse, covering the alkyl CH, aromatic CH, and OH stretch regions of the infrared.

The experimental spectra are compared with the predictions of calculations carried out on optimized structures of the low-energy conformers of the molecules of interest. Starting structures for the geometry optimizations were generated from a conformational search using the AMBER force field in the MacroModel program suite. All structures within 50 kJ/mol of the global minimum (∼20−40 conformational minima) were used as starting structures for subsequent geometry optimizations. Initial optimizations were carried out using density functional theory (DFT) with the Becke3LYP functional and a 6-31+G(d) basis set. Low energy structures from these optimizations were then reoptimized using dispersion-corrected density functional (ωB97X-D, M05-2X, and M06-2X) using the same basis set. For the structures of interest here, no large changes in relative energy were observed between the methods. Ground state frequencies were calculated with B3LYP/6-31+G* level of theory with an ultrafine grid and tight optimization. Time-dependent DFT (TD-DFT) calculations of vertical excitation energies were calculated using both B3LYP and M06-2X functionals. All the density functional theory computations were carried out using the Gaussian 09 suite of programs.[20]

3. RESULTS AND ANALYSIS

3.A. Conformational Preferences of Simpler Lignin Analogues. Of the three monolignols, *p*-coumaryl alcohol is the

root structure (Figure 1a), to which one methoxy group (coniferyl alcohol, Figure 1b) or two methoxy groups (sinapyl alcohol, Figure 1c) are added at the positions ortho to the OH group on the ring. In seeking to understand the conformational preferences of these molecules, with their multiple substituents, it is helpful at the outset to review what is known about the conformational preferences of simpler molecules containing these substituents. Predictions based on these simpler lignin analogues can be used to sort through the various possibilities for the monolignols themselves.

The jet-cooled infrared and ultraviolet spectra of *p*-vinylphenol (*p*VP) and *o*-methoxyphenol (*o*MP) have been studied previously.[14,16]

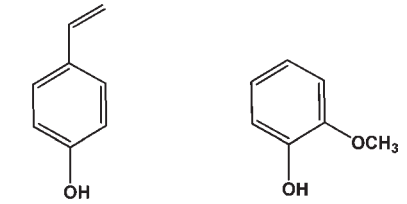

p-vinylphenol (*p*VP) *o*-methoxyphenol (*o*MP)

*p*VP differs from *p*CoumA in lacking the CH_2OH group present in the latter. Under jet-cooled conditions, *p*VP spreads its population roughly equally over two conformers, with a splitting between their S_0-S_1 origin transitions of just 4 cm^{-1}. High resolution UV scans of the rotational structure were used by Morgan et al.[14] to prove that *p*VP is planar in both S_0 and S_1 states. Small differences in the rotational constants were used by these authors to assign the *anti* conformer, with vinyl and OH groups pointing in opposite directions, as the red member of the doublet and *syn* to the blue member.

*o*MP has OH and methoxy groups ortho to one another on the aromatic ring, as occurs in ConA (Figure 1b). Under jet-cooled conditions, *o*MP funnels all of its population into a single conformation in which the OH group engages in a H-bond with the methoxy oxygen. IR spectra of this conformer showed an OH stretch fundamental shifted down from its free position (3654-7 and 3661-2 cm^{-1} in *m*- and *p*-methoxyphenol rotational isomers)[16] to 3599 cm^{-1}, proving the presence of this intramolecular H-bond.

3.B. Electronic Spectroscopy of *p*-Coumaryl Alcohol (*p*CoumA). The fluorescence excitation spectrum of *p*CoumA is shown in Figure 2. All the transitions of the spectrum are split into doublets separated by approximately 7 cm^{-1}. UVHB spectroscopy (not shown) was used to confirm that the two members of the doublet belong to two different conformations, with intensities similar to one another. In this sense, the spectroscopy of *p*CoumA is closely analogous to that of *p*VP, with its 4 cm^{-1} splitting.[13,14] In *p*CoumA, the two conformational origins were observed at 33127/33134 cm^{-1}, a shift of about 80 cm^{-1} to the red relative to *p*VP (33207/33211 cm^{-1}).

DFL spectra carried out on vibronic transitions of the two conformers showed that the two members of each doublet in the excitation spectrum had nearly identical spectra. As an example, Figure 3 compares the DFL spectra of the S_0-S_1 origin transitions of the two conformers.

Taken together, the spectral data lead to an assignment of the two observed conformers of *p*CoumA as a *syn*/*anti* pair (Figure 4a), much as in *p*VP, differing from one another in the relative orientations of the vinyl and OH groups. We cannot make firm assignments on the basis of the data at hand as to which member of the doublet to assign as *syn* or *anti*, although the analogy with *p*VP would suggest that the red-shifted member of the doublet is most likely *anti* and the blue member *syn*. The presence of only two conformations and the close analogy with *p*VP lead to the conclusion that the $CH{=}CH-CH_2OH$ group is locked into a single conformation.

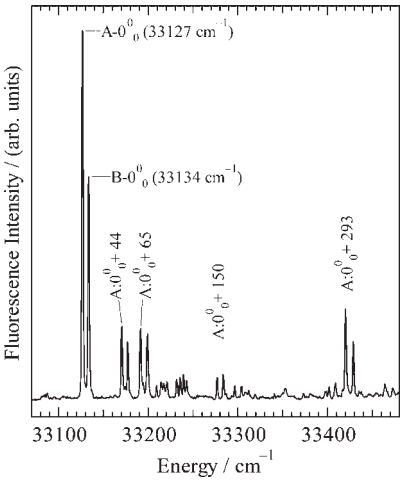

Figure 2. Fluorescence excitation spectrum of jet-cooled *p*-coumaryl alcohol.

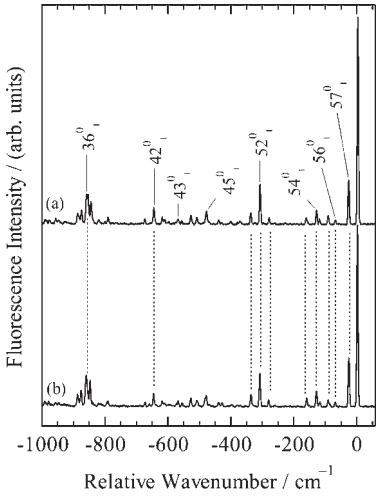

Figure 3. S_1 origin DFL spectra of (a) conformer A and (b) conformer B of *p*-coumaryl alcohol. See Table 1 for details of the assignments.

Calculations of the low-energy conformers of *p*CoumA are in keeping with these deductions. At all levels of theory investigated (DFT B3LYP/6-31+G(d), DFT M06-2X/6-31+G(d)), the two structures shown in Figure 4a, which form a *syn*/*anti* pair, are significantly lower in energy than all others. Figure 5a shows a representative energy level diagram of the 10 lowest energy structures of *p*CoumA at the B3LYP/6-31+G(d) level of theory, where the energy gap is about 4 kJ mol^{-1}. These two structures share the same conformation for the CH_2OH group, in which the oxygen atom is out-of-plane and the OH group is oriented so that its hydrogen points out over the vinyl group π cloud. In so doing, the OH group breaks the plane of symmetry for reflection

dx.doi.org/10.1021/ja109218j |*J. Am. Chem. Soc.* 2011, 133, 2632–2641

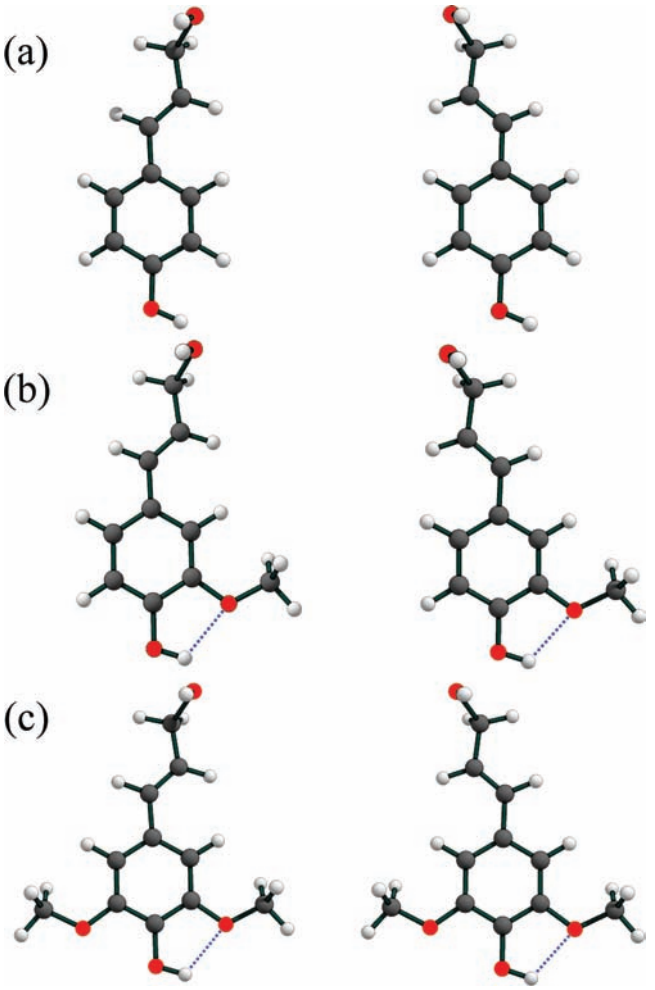

Figure 4. Two lowest energy calculated structures of (a) *p*CoumA, (b) ConA, and (c) SinA. In each case, the two structures form a *syn*/*anti* pair, differing in the relative orientations of the OH and vinyl groups relative to one another.

through the aromatic ring plane. We will consider the reasons for this preferred conformation of the CH_2OH group in the Discussion.

This symmetry breaking is evident in the Franck−Condon activity of the low-frequency vibronic transitions, where the fundamentals of several (nominally) out-of-plane fundamentals appear in the spectrum (Table 1). The frequencies calculated with B3LYP/6-31+G* match quite closely with the experimental values, supporting the assignment of the two lowest energy structures to the *syn*/*anti* pair shown in Figure 4a. Notably, the prominent band (57_1^0) at 29 cm^{-1} in the DFL spectra of Figure 3 is assigned as the fundamental of the out-of-plane vinyl torsion, calculated at 29 cm^{-1} (Table 1). This same vibration is seen only as even overtones in styrene[21] and *p*VP,[13] where planarity is retained. The fundamentals of several other out-of-plane torsions and bends are also Franck−Condon active, confirming the symmetry breaking present in the structures shown in Figure 4a.

3.C. Coniferyl Alcohol (ConA) and *o*-Methoxy-*p*-vinylphenol (MVP) Spectroscopy. Coniferyl alcohol (ConA, Figure 1b) and *o*-methoxy-*p*-vinylphenol (MVP) are close analogues of one another, with MVP lacking only the CH_2OH group present in ConA. As a result, we studied the single-conformation spectroscopy

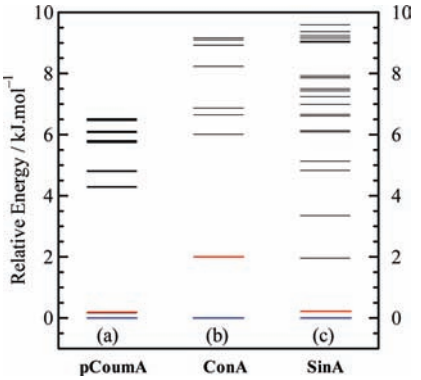

Figure 5. Energy level diagrams of the low-energy conformers of (a) *p*CoumA, (b) ConA, and (c) SinA. The two lowest energy structures of each monomer, the *syn* (blue) and *anti* (red) conformers, are shown in Figure 4. All ConA and SinA structures shown here have an intramolecular OH···OCH_3 H-bond. Structures of ConA without an intramolecular H-bond are destabilized by at least 10 kJ mol^{-1} relative to the global minimum.

Table 1. Assigned Experimental and Calculated Frequencies (cm^{-1}) for *p*CoumA with Mode Descriptions

mode[a]	S_1[b] calcd/exptl	mode[a]	S_0[c] calcd/exptl	description[e]
57	47/44	56	71/71	β oop
56	62/66	54	128/131	$\tau(CH_2OH)$
55	105/105	55	100/93	t(−C═C−OH)
54	150/151	53	209/−	β oop
53[d]	197/−	57[d]	29/29	τ(Ph−C═C) oop
52	294/−	49	352/−	$\tau(OH_{phenol})$
51	317/294	52	303/310	$\tau(OH_{vinyl})$

[a] Mulliken mode numbering used. [b] Calculated at the CIS/6-31+G* level of theory. [c] Calculated at the DFT B3LYP/6-31+G* level of theory. [d] Corresponds to the vinyl torsion (ν_{42}) of styrene. [e] t: twisting. τ: torsion. β: bend. oop: out-of-plane.

of both molecules with an eye toward using the results on MVP to guide our interpretation of the spectra of ConA.

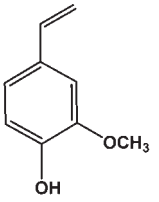

o-methoxy-*p*-vinylphenol
(MVP)

Not unexpectedly, the same *syn* and *anti* conformers identified in *p*CoumA are also calculated to be the two lowest energy structures in ConA and MVP, here with the single methoxy group on the ring locking in the OH conformation in an intramolecular H-bond (Figure 4b), much as it is in *o*-methoxyphenol,[16] and enhancing the energy difference between the *syn* and *anti* conformers (Figure 5b). In ConA, these two conformers are calculated to be 4 kJ mol^{-1} lower in energy than all other conformers, with *syn* 2 kJ mol^{-1} below *anti* and all structures in the lowest 10 kJ mol^{-1} possessing an OH···OCH_3

dx.doi.org/10.1021/ja109218j |*J. Am. Chem. Soc.* 2011, 133, 2632–2641

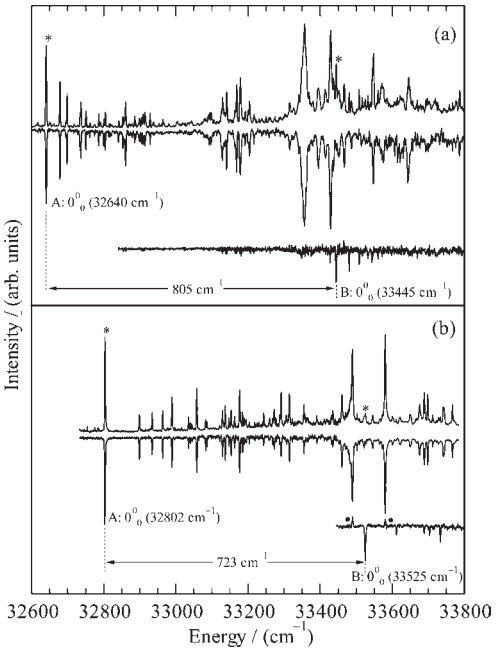

Figure 6. FES, UVHB spectra of (a) ConA and (b) MVP. Transitions marked with asterisks were used as hole-burning transitions. False peaks marked with solid circles in the UVHB spectra arise from incomplete subtraction when large transitions due to another conformer are encountered.

H-bond. TDDFT vertical excitation energies (Table 3) for the S_0-S_1 transitions in MVP and ConA predict *syn*/*anti* splittings of 636 and 419 cm^{-1}, respectively, with *anti* blue-shifted relative to *syn* in both molecules.

The top traces in Figures 6a and Figure 6b show the fluorescence excitation spectra of ConA and MVP, respectively, over the 32600−33800 cm^{-1} region. The bottom two traces in each case show the corresponding UVHB spectra, proving the presence of two conformers of each. The spectra of the two molecules bear a strong resemblance to one another, with a major conformer (conformer A) with S_0-S_1 origins at 32640/32802 cm^{-1} and with a minor conformer (B) with transitions about 5 times less intense with origins at 33445/33525 cm^{-1}. This blue shift of 805/723 cm^{-1} in the two molecules is over 100 times larger than the splitting in *p*CoumA and *p*VP, which lack the methoxy group ortho to the OH on the ring. On the basis of a comparison with the TDDFT calculations, we tentatively assign conformer A of MVP and ConA to their respective *syn* structures and assign conformer B to *anti*.

Figure 7a,b shows the FDIR spectra of the two conformers of ConA in the OH stretch region, while Figure 7c,d shows the corresponding spectra for MVP. All four conformers have aromatic OH stretch fundamentals just below 3600 cm^{-1} and within a few cm^{-1} of one another. This frequency is nearly identical to that in *o*MP (3599 cm^{-1}), proving that the observed conformers of both ConA and MVP have an intramolecular OH···OCH_3 H-bond, as in *o*MP,[16] and consistent with the structures assigned. The FDIR spectra of both conformers of ConA (Figure 7a) also show an OH stretch fundamental due to the CH_2OH group at 3652 cm^{-1}, consistent with the position of a free alkyl OH stretch, as in benzyl alcohol (3650 cm^{-1}).[22] The apparent splitting of this band is due to absorption of the IR by atmospheric moisture.

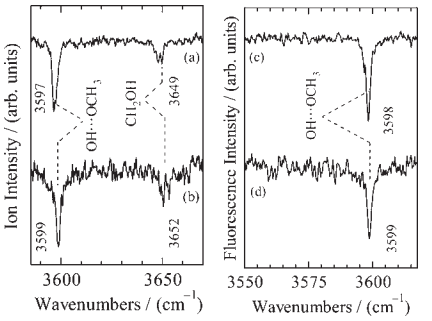

Figure 7. (a, b) RIDIR spectra of ConA (a) conformer A and (b) conformer B in the OH stretch region. (c, d) FDIR spectra of MVP conformers (c) A and (d) B.

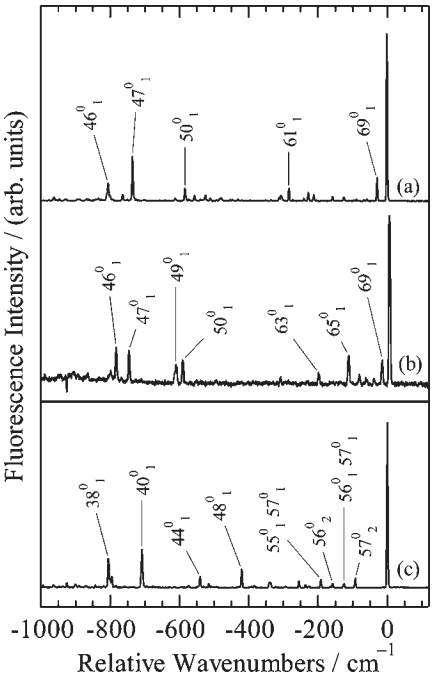

Figure 8. S_1 origin DFL spectra of (a) conformer A, (b) conformer B of ConA, and (c) conformer A of MVP. The corresponding spectrum of conformer B of MVP was not recorded because of spectral congestion in the FE spectrum. See Table 2 for details of the assignments.

Figure 8a,b presents DFL spectra of the S_0-S_1 origins of conformers A and B of ConA, while Figure 8c shows the corresponding spectrum for conformer A of MVP. The spectrum of conformer B of MVP was not recorded because of interference from transitions due to conformer A in this congested region of the FE spectrum (Figure 6b).

Several pieces of evidence from the DFL spectra support an assignment of conformer A of ConA and MVP as the *syn* and conformer B as the *anti* structures shown in Figure 5b. In MVP, the lowest frequency vibronic band in the DFL spectrum is at 92 cm^{-1} while the corresponding lowest frequency bands in the spectra of the *syn* and *anti* conformers of ConA appear at 28 and 20 cm^{-1}, respectively. Since MVP is anticipated to retain planarity in both S_0 and S_1 states, out-of-plane fundamentals should be dipole-forbidden. As anticipated, the lowest frequency vibration in MVP is the vinyl torsion, an a″ mode of 46 cm^{-1} (Table 2), precisely one-half the experimentally observed value.

Table 2. Ground State Frequencies of ConA and MVP with Computed Frequencies of *syn*/*anti* Pairs[a]

coniferyl alcohol (ConA)					*o*-methoxy-*p*-vinylphenol (MVP)				
origin SVLF freq (obsd)/ cm^{-1}		B3LYP/6-31+G(d) freq (calcd)/cm^{-1} scaled by 0.99			origin SVLF freq (obsd)/ cm^{-1}		B3LYP/6-31+G(d) freq (calcd)/cm^{-1} scaled by 0.99		
Conf A	Conf B	*syn*	*anti*	mode/symm	Conf A	Conf B[b]	*syn*	*anti*	mode/symm
28	20	28	26	69/a	46[c]		46	54	57/a″
582	597	589	605	50/a	79[c]		82	76	56/a″
	614	615	617	49/a	421		419	404	48/a′
734	752	740	759	47/a	540		539	553	44/a′
804	789	813	803	46/a	709		707	712	40/a′
					805		804	803	38/a′

[a] Relatively strong transitions were used. [b] DFL data not available. [c] Half of the experimental frequency (overtone) is shown here, since the fundamental transition is forbidden.

The higher frequency in-plane ring fundamentals at 421, 540, 709, and 805 cm^{-1} in the spectrum of MVP(A) are close matches with the calculated frequencies for the *syn* conformer and significantly better than the match with the *anti* structure. The corresponding transitions in ConA confirm these assignments, with both low-frequency fundamentals (now allowed because of the out-of-plane CH_2OH group) and in-plane ring fundamentals showing an excellent match of A with *syn* and B with *anti*.

In summary, both ConA and MVP have their population spread over only two conformers, a dominant conformer with S_0-S_1 origin near 32640/32802 cm^{-1} assigned to the *syn* structure (Figure 4b) and a minor conformer shifted nearly 800 cm^{-1} to the blue assigned to the *anti* conformer. The close correspondence between the spectroscopy of the two molecules confirms and strengthens the assignments in both molecules.

3.D. Spectroscopy of Sinapyl Alcohol. Figure 9 presents the fluorescence excitation spectrum of SinA and two UVHB spectra with hole-burn laser fixed on transitions marked by the filled circles in the figure. Apart from a minor interference from transitions due to thermal degradation/polymerization that does not appear in the mass-resolved R2PI spectrum (marked with asterisks), all transitions can be ascribed to two conformers of SinA, with S_0-S_1 origin transitions at 33 055 cm^{-1} (conformer A) and 33 294 cm^{-1} (conformer B), a splitting of 239 cm^{-1}. The similar intensities of the two origin transitions suggest that the two conformers split the population of SinA roughly equally between them.

Figure 4c shows the structures for the two lowest-energy conformers, which again form a *syn*/*anti* pair. Here the addition of a second methoxy group at the other ortho position on the ring has made the two conformers nearly isoenergetic, with the *syn* conformer only 0.2 kJ mol^{-1} more stable than *anti* (Figure 5c). Given the subtle differences in vibronic spectra of the two conformers, we do not have an unequivocal assignment of which is *syn* and which is *anti*. However, the firm assignment of the red-shifted conformer to *syn* and blue-shifted to *anti* in ConA and MVP suggests a similar assignment here. Vertical excitation energies calculated at the TDDFT B3LYP/6-31+G(d) level of theory are consistent with this choice (Table 3).

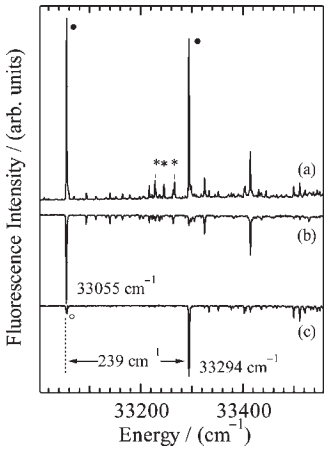

Figure 9. (a) FE spectrum and (b, c) UVHB spectra of (b) conformer A and (c) conformer B of sinapyl alcohol (SinA). The S_0-S_1 origins of the two conformers are separated by 239 cm^{-1}. Asterisks denote transitions arising from thermal degradation products. Peaks labeled with solid circles were used as hole-burn transitions in the UVHB experiment. Incomplete subtraction is responsible for the small interference signal (open circle) from conformer A in the UVHB spectrum of B.

4. DISCUSSION

4.A. Conformational Preferences of the Monolignols. The spectroscopic results presented here have led to assignments for the low-energy conformers of the three monolignols *p*-coumaryl alcohol, coniferyl alcohol, and sinapyl alcohol. In each case, only two conformers were observed, which have been assigned to the *syn*/*anti* pairs shown in Figure 4. In *p*CoumA and SinA, these two conformers had similar populations, while in ConA, transitions due to the *syn* conformer were about 5 times more intense than those due to *anti*. Thus, despite the presence of multiple flexible substituents (OH, OCH_3, allyl alcohol), all three monolignols show clear conformational preferences that lock in and stabilize one or at most two conformations relative to all others.

In accounting for these preferences, it is worthwhile to consider the conformational preferences of a series of simpler lignin analogues containing some subset of the substituents present in the monomers themselves. Figure 10 presents a series of molecules that can serve this purpose.

Previous studies of phenol,[23,24] anisole,[25] and styrene[21,26] have proven that the OH, OCH_3, and vinyl substituents all prefer in-plane structures that enable conjugation of the oxygen lone pair or vinyl π cloud with the aromatic ring. *p*-Vinylphenol (Figure 10a, left) brings together the vinyl and OH substituents in the same molecule. As anticipated, this preference for planarity is retained

Table 3. Calculated Vertical Excitation Energies for the $S_1 \leftarrow S_0$ Transitions of the Indicated Molecules

molecule/conformer	TD/B3LYP/6-31+G(d) single point energies/cm^{-1}	S_1-S_0 vertical splitting (calcd)/ cm^{-1} $\Delta E(anti-syn)$	S_1-S_0 origin separation (exptl)/cm^{-1} $\Delta E(anti-syn)$
*p*CoumA/*syn*	35 712	+88	−7
*p*CoumA/*anti*	35 800		
MVP/*syn*	34 892	+ 636	+723
MVP/*anti*	35 528		
ConA/*syn*	34 339	+419	+805
ConA/*anti*	34 758		
SinA/*syn*	33 499	+186	+239
SinA/*anti*	33 685		

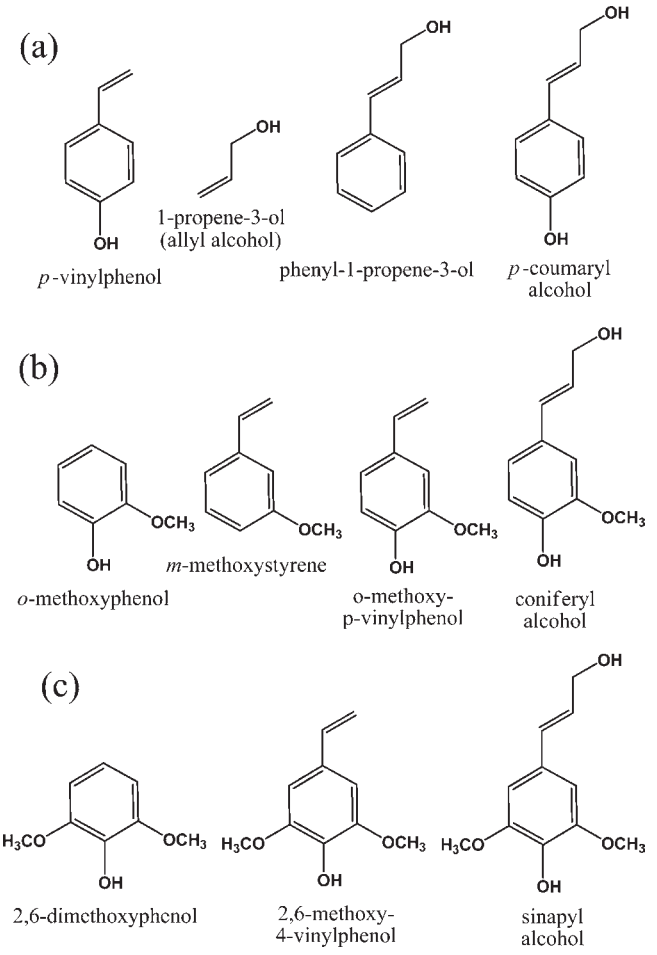

Figure 10. (a) Chemical structures: (a) *p*-vinylphenol, 1-propene-3-ol (allyl alcohol), 1-phenyl-1-propene-3-ol, and *p*-coumaryl alcohol (*p*CoumA); (b) *o*-methoxyphenol, *m*-methoxystyrene, *o*-methoxy-*p*-vinylphenol (MVP), and ConA; (c) 2,6-dimethoxyphenol, 2,6-dimethoxy-4-vinylphenol, and sinapyl alcohol (SinA).

upon para substitution, as proven by the vibronic and rotationally resolved spectroscopy on the molecule by the groups of Buma[13] and Pratt.[14] The asymmetry of the vinyl group distinguishes the two in-plane positions of the OH group, just sufficiently to split the S_0-S_1 origins; however, the spectroscopy of the two conformers is otherwise nearly identical. *p*CoumA (Figure 10a, right) also has an isolated OH group para to the vinyl group. Figure 11a presents a relaxed potential energy scan for internal rotation of the phenol OH group of *p*CoumA, showing the two nearly equivalent in-plane

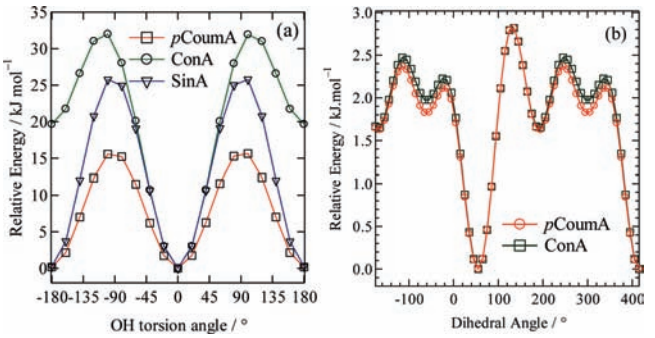

Figure 11. Relaxed potential energy scans for internal rotation about the (a) phenolic C−O bond and (b) the C−O bond of the CH_2OH group in the indicated molecules.

minima and barriers at the perpendicular configuration of ~15.6 kJ mol^{-1} (1300 cm^{-1}).

When OH and OCH_3 substituents are placed ortho to one another on the ring, as in *o*-methoxyphenol (Figure 10b, left), the two substituents also remain in-plane, with a fixed orientation in which the OH forms a hydrogen bond to the methoxy oxygen. This preference is retained in both MVP and ConA, as proven by their OH stretch RIDIR spectra (section 3.C). We have carried out calculations on *o*MP, MVP, and ConA that confirm a strong energetic preference for this configuration. The relaxed potential energy scan for hindered rotation of the OH group in ConA is shown in Figure 11a. The H-bonded configuration is 19.6 kJ mol^{-1} more stable than the secondary minimum with the OH pointing away from the methoxy group. Thus, the combined presence of OH and OCH_3 groups enhances the in-plane preference but locks the OH to the OCH_3 group.

When a second OCH_3 group is added at the 6-position (Figure 10c, left), the in-plane preference is retained, but the two orientations of the OH group are now equivalent, forming H-bonds to one or the other methoxy group. In 2,6-dimethoxy-4-vinylphenol (Figure 10c, middle), the symmetry is broken by the asymmetric vinyl group across the ring. This same weak symmetry breaking is present in SinA (Figure 10c, right), here enhanced somewhat by the CH_2OH group. The relaxed potential energy scan for OH internal rotation of SinA (Figure 11a bears this out, with a calculated energy difference for the *syn* and *anti* conformers of only 0.22 kJ mol^{-1}.

In the monolignols, the vinyl substituent is modified to propene-3-ol (allyl alcohol) by adding a CH_2OH to it in the *trans* configuration. We have shown that the OH group breaks the plane of symmetry of the vinyl group, making the fundamentals of all low-frequency vibrations allowed in all three molecules. We surmise on

dx.doi.org/10.1021/ja109218j |*J. Am. Chem. Soc.* 2011, 133, 2632–2641

this basis that the oxygen atom is brought out-of-plane. The orientation of the OH group is not pinned down unequivocally by the data; however, a single orientation is observed in all three molecules.

In order to assess the preferred orientation of the OH group, we carried out relaxed potential energy scans for internal rotation about the C−O bond in *p*CoumA and ConA. The results, shown in Figure 11b, indicate a strong preference for a conformation in which the OH group points the hydrogen back over the vinyl π cloud, with only shallow minima at other configurations. This preference is one that holds already in allyl alcohol (Figure 10a, middle), as proven by microwave studies that utilized Kraitchman analysis to locate the position of the hydrogen atom.[27] Indeed, we have carried out a full 2D relaxed potential energy scan on allyl alcohol that confirms the strong preference for both out-of-plane oxygen and gauche OH orientation (Figure S1, Supporting Information).

At first glance, the preference for an OH orientation that points the hydrogen back over the π cloud would seem to reflect a weak H-bond stabilizing this orientation. Indeed, natural bond order (NBO) analysis does locate a possible interaction between the vinyl π orbital and the H−O σ^* antibonding orbital (Figure S2, Supporting Information). However, this interaction is calculated to be exceedingly weak and thus seems incapable of accounting for the strong energetic preference shown in Figure 11b. Instead, the relaxed scan shows that all other orientations for the OH group are destabilized to a similar extent, suggesting that a better description of the orientational preference is that it minimizes the repulsions between the oxygen lone pairs and the vinyl π cloud that destabilize the other minima in Figure 11b. Thus, the entire $-CH{=}CH-CH_2OH$ group has a strong preference for a single conformation. Furthermore, the local minima in Figure 11b have small barriers (<1 kJ/mol) that are insufficient to trap population behind them, facilitating collisional cooling into the most stable conformation.

This, when combined with the locking of the OH and OCH_3 groups (when present), produces just two conformers of each of the three monolignols, which are *syn*/*anti* pairs involving the relative orientation of the vinyl and OH groups para to one another on the ring. While in *p*CoumA and SinA the *syn* and *anti* conformations are nearly isonergetic, in ConA, the asymmetry of the ring produces a modest energy difference (~2 kJ mol^{-1} via calculation) that leads nevertheless to a 5:1 intensity ratio of *syn* over *anti*, producing a single dominant conformation. Thus, despite the presence of several flexible substituents, the monolignols are structurally quite rigid.

4.B. Spectroscopic Signatures. One of the goals of the present study was to determine the spectroscopic signatures of the three monolignols as a foundation for future studies of larger lignin oligomers. We hypothesize that there may be a role for UV spectroscopy of this aromatic-laden biopolymer lignin in sequencing larger oligomers. The present data highlight the sensitivity of the position of the S_0-S_1 electronic origin to the particular lignin monomer and even to the *syn*/*anti* conformer. Figure 12 presents a simple stick diagram of the wavenumber positions and relative intensities of the S_0-S_1 origins of the *syn* and *anti* conformers of the three monolignols. As is evident from this figure, the small splitting (7 cm^{-1}) present in *p*CoumA is about a central position of 33 130 cm^{-1}, which serves as an approximate center for the much larger splittings present in the other two molecules as well. In ConA, the asymmetry of the $OH\cdots OCH_3$ group magnifies this splitting to 805 cm^{-1}, with origins positioned −490 and +315 cm^{-1} from the central position. In SinA, the introduction of a second methoxy group, with its more nearly symmetric configuration, reduces the splitting to 239 cm^{-1}, with positions −75 and +164 cm^{-1} from center. These splittings are reflected qualitatively by the calculated vertical energies for the *syn* and *anti* conformers of the three molecules, which are collected together with the experimental splittings in Table 3. While the absolute magnitudes of the calculated splittings are only about half the experimental values, the relative sizes of the splittings faithfully follow the experimental trends.

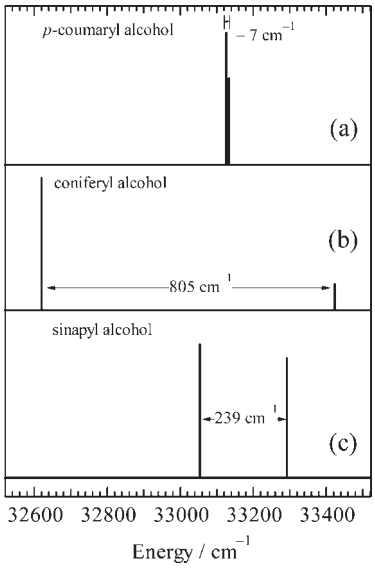

Figure 12. Stick diagrams of the wavenumber positions (cm^{-1}) and relative intensities of the $S_1 \leftarrow S_0$ origin transitions of *syn* (red-shifted) and *anti* (blue-shifted) conformers of (a) *p*CoumA, (b) ConA, and (c) SinA. In *p*CoumA, −7 cm^{-1} indicates that the *anti* isomer is red-shifted from *syn*.

Of the three substituents (vinyl, OH, OCH_3), the vinyl group is directly conjugated with the ring and imposes the greatest asymmetry on the ring. The tiny splitting present in *p*CoumA (7 cm^{-1}) indicates that the OH group by itself has almost no effect in producing an electronic asymmetry between *syn* and *anti* conformations. Given the dramatic increase in splitting in ConA, it seemed likely to us that it was the methoxy group in the meta position that was linked most directly to the vinyl group and sensitive to its orientation. However, calculations carried out on *m*-methoxystyrene (Figure 10b, middle) predict a splitting of only 91 cm^{-1} between the *syn* and *anti* conformers while the calculated splitting in MVP (636 cm^{-1}) is 7 times larger. We surmise on this basis that it is the combined effect of *p*-OH and *m*-OCH_3 groups, when H-bonded to one another, that produces the large splitting observed for ConA. The resulting stabilization of the *syn* conformer relative to *anti* in the S_1 state will mean that the conformational potential energy surface will look quite different in S_1 than in S_0, a point worth further investigation by theory.

Finally, besides these electronic effects, the positions and types of substituents on the rings influence the ring-mode frequencies and Franck−Condon activities in characteristic ways that can be used to distinguish the lignin monomer responsible for the emission. The S_1 origin DFL spectra of the *syn* conformers of *p*CoumA (Figure 3a), ConA (Figure 8a), and SinA (Figure S3) show strong activity in ring fundamentals that can be identified and assigned as ring deformation modes (nominally 6a and 6b)

Table 4. Ground State Ring Deformation Vibrational Modes of the Monolignols

	experimental frequencies/cm^{-1}		
molecule (confomer A)	$6a_1$ [a]	$6b_1$ [a]	1_1 [a]
*p*CoumA	570 (43_1)	647(42_1)	847 (36_1)
ConA	582 (50_1)	734 (47_1)	804 (45_1)
SinA	534 (59_1)	925 (53_1)	815 (49_1)

[a] Vibrational numbering using the Varsanyi numbering scheme.[25] Mulliken mode numbers are given in parentheses.

and ring breathing modes (1) according to the Varsanyi vibrational numbering scheme for benzene derivatives.[24,28] The Franck−Condon activity in these vibrations is at times spread over more than one transition because of mixing with other modes in the molecule. Furthermore, the assignment as 6a versus 6b has less meaning in asymmetric derivatives. Nonetheless, the identification of vibrations that contains these motions and the match-up between experimental and calculated frequencies are excellent, providing a basis of assignment for much of this activity. Table 4 highlights this comparison for the $6a_1^0$, $6b_1^0$, and 1_1^0 transitions of the three monolignols. In the table, both the Varsanyi[28] and Mulliken[29] numbering schemes are given. A striking aspect of the three spectra is the increasing splitting between the 6a and 6b pair, due in large measure to an increase in frequency of the (nominal) $6b_1^0$ fundamental to the point that it appears above the 1_1^0 fundamental in SinA. In addition, the $\pi-\pi^*$ transition studied here shows Franck−Condon activity and Duschinsky mixing in the low frequency vibrations that is characteristic of the vinyl group, here extended to the longer allyl alcohol side chain.

5. CONCLUSIONS

Single-conformation spectroscopy of the three monolignols *p*-coumaryl alcohol, coniferyl alcohol, and sinapyl alcohol has shown them to be structurally quite rigid, producing in each case only two conformers that form a simple *syn*/*anti* pair describing the relative orientations of the OH and vinyl groups on the ring. When present, the intramolecular H-bond between OH and methoxy groups locks in their relative orientation. The potentially flexible −CH═CH−CH_2OH group also shows a distinct preference for a single position and orientation for the remote OH group, out-of-plane, with hydrogen pointing back over the vinyl group.

The UV spectroscopy of these molecules is sensitive to the number and position of the methoxy groups on the ring, primarily in modulating the splitting between the S_0-S_1 origins of the *syn* and *anti* conformers by over a factor of 100. Since ConA also has a distinct energetic preference for the *syn* conformer, its electronic spectrum is dominated by this single conformer, which is shifted several hundred cm^{-1} red of all others. One can anticipate a similar sensitivity of the electronic spectrum of larger oligomers to the chemical linkage between them and the relative positions of the monomer units along the chain.

A final important conclusion of this work is the experimental challenge already presented by these monolignols for study in the gas phase. Commercial samples of the monomers were extraordinarily sensitive to thermal or UV-induced polymerization. In order to get the samples into the gas phase, the samples required heating that led to thermal polymerization inside the heated sample cylinder. This sensitivity to temperature may have been responsible for the mistaken deduction of previous workers that one-color R2PI spectra of ConA was not possible.[2] This suggests that laser desorption may be needed to extend these studies to larger lignin oligomers, a task we are currently pursuing.

■ ASSOCIATED CONTENT

Supporting Information. (1) Experimental details of sample handling, (2) further discussion of the conformational preferences of the allyl alcohol side chain, including a relaxed 2D scan of the allyl alcohol dihedral angles, (3) description of the natural bond orbital analysis (NBO) of allyl alcohol, and (4) DFL spectra of the S_1 origins of the two conformers of SinA. This material is available free of charge via the Internet at http://pubs.acs.org.

■ AUTHOR INFORMATION

Corresponding Author
zwier@purdue.edu

■ ACKNOWLEDGMENT

This work was supported by the Department of Energy Basic Energy Sciences, Division of Chemistry, under Grant DE-FG02-96ER14656. The authors gratefully acknowledge Dr. Joshua J. Newby for help with some of the DFL spectra of MVP, and Jacob Dean for recording R2PI spectra of sinapyl alcohol and *p*-coumaryl alcohol that confirmed the monolignols as carriers of the fluorescence-based data.

■ REFERENCES

(1) Evtuguin, D. V.; Amado, F. M. L. *Macromol. Biosci.* **2003**, *3* (7), 339.
(2) Hage, E. R. E. v. d.; Boon, J. J.; Steenvoorden, R. J. J. M.; Weeding, T. L. *Anal. Chem.* **1994**, *66*, 543.
(3) Reale, S.; Tullio, A. D.; Spreti, N.; Angelis, F. D. *Mass Spectrom. Rev.* **2004**, *23*, 87.
(4) Syrjänen, K.; Brunow, G. *J. Chem. Soc., Perkin Trans. 1* **2000**, 183.
(5) DellaGreca, M.; Iesce, M. R.; Previtera, L.; Purcaro, R.; Rubino, M.; Zarrelli, A. *Photochem. Photobiol. Sci.* **2008**, *7*, 28.
(6) Kishimoto, T.; Uraki, Y.; Ubukata, M. *Org. Biomol. Chem.* **2005**, *3*, 1067.
(7) Houtman, C. J. *Holzforschung* **1999**, *53* (6), 585.
(8) Boerjan, W.; Ralph, J.; Baucher, M. *Annu. Rev. Plant Biol.* **2003**, *54*, 519–546.
(9) Vanholme, R.; Morreel, K.; Ralph, J.; Boerjan, W. *Curr. Opin. Plant Biol.* **2008**, *11* (3), 278–285.
(10) Lewis, N. G.; Inciong, M. E. J.; Dhara, K. P.; Yamamoto, E. *J. Chromatogr.* **1989**, *479* (2), 345.
(11) Lewis, N. G.; Inciong, M. E. J.; Ohashi, H.; Towers, G. H. N.; Yamamoto, E. *Phytochemistry* **1988**, *27* (7), 2119–2121.
(12) Steeves, V.; Forster, H.; Pommer, U.; Savidge, R. *Phytochemistry* **2001**, *57* (7), 1085–1093.
(13) de Groot, M.; Buma, W. J.; Gromov, E. V.; Burghardt, I.; Köppel, H.; Cederbaum, L. S. *J. Chem. Phys.* **2006**, *125*, 204303.
(14) Morgan, P. J.; Mitchell, D. M.; Pratt, D. W. *Chem. Phys.* **2008**, *347* (1−3), 340.
(15) Smolarek, S.; Vdovin, A.; Perrier, D. L.; Smit, J. P.; Drabbels, M.; Buma, W. J. *J. Am. Chem. Soc.* **2010**, *132* (18), 6315.
(16) Fujimaki, E.; Fujii, A.; Ebata, T.; Mikami, N. *J. Chem. Phys.* **1999**, *110* (9), 4238.
(17) Wei, K.; Luo, S.-W.; Fu, Y.; Liu, L.; Guo, Q.-X. *J. Mol. Struct.: THEOCHEM* **2004**, *712*, 197.

(18) Pillsbury, N. R.; Müller, C. W.; Meerts, W. L.; Plusquellic, D. F.; Zwier, T. S. *J. Phys. Chem. A* **2009**, *113* (17), 5000.
(19) Zwier, T. S. *J. Phys. Chem. A* **2001**, *105* (39), 8827.
(20) Frisch, M. J.; et al. *Gaussian 09*, revision A.1; Gaussian, Inc.: Wallingford, CT, 2009.
(21) Syage, J. A.; Adel, F. A.; Zewail, A. H. *Chem. Phys. Lett.* **1983**, *103* (1), 15.
(22) Miller, B. J.; Kjaergaard, H. G.; Hattori, K.; Ishiuchi, S.-i.; Fujii, M. *Chem. Phys. Lett.* **2008**, *466* (1−3), 21.
(23) Schumm, S.; Gerhards, M.; Kleinermanns, K. *J. Phys. Chem. A* **2000**, *104* (46), 10648.
(24) Roth, W.; Imhof, P.; Gerhards, M.; Schumm, S.; Kleinermanns, K. *Chem. Phys.* **2000**, *252* (1−2), 247.
(25) Matsumoto, R.; Sakeda, K.; Matsushita, Y.; Suzuki, T.; Ichimura, T. *J. Mol. Struct.* **2005**, *735*−*736*, 153.
(26) Grassian, V. H.; Bernstein, E. R.; Secor, H. V.; Seeman, J. I. *J. Phys. Chem. A* **1989**, *93*, 3470.
(27) Murty, A. N.; Curl, R. F. *J. Chem. Phys.* **1967**, *46* (11), 4176.
(28) Varsanyi, G. *Assignments for Vibrational Spectra of 700 Benzene Derivatives*; Wiley: New York, 1974.
(29) Mulliken, R. S. *J. Chem. Phys.* **1955**, *23*, 1997.